

Scanning tunneling microscopic studies of platinum electrode surfaces

Fu Ren F. Fan, and Allen J. Bard

Anal. Chem., 1988, 60 (8), 751-758 • DOI: 10.1021/ac00159a005

Downloaded from <http://pubs.acs.org> on February 2, 2009

More About This Article

The permalink <http://dx.doi.org/10.1021/ac00159a005> provides access to:

- Links to articles and content related to this article
- Copyright permission to reproduce figures and/or text from this article



ACS Publications
High quality. High impact.

Analytical Chemistry is published by the American Chemical Society. 1155 Sixteenth Street N.W., Washington, DC 20036

Scanning Tunneling Microscopic Studies of Platinum Electrode Surfaces

Fu-Ren F. Fan and Allen J. Bard*

Department of Chemistry, University of Texas, Austin, Texas 78712

Scanning tunnelling microscopy (STM) was applied in air to studies of the topography of different Pt surfaces (polycrystalline, single crystal, Pt sputtered on mica) after different pretreatments. Ripple structures found when scanning the surface of atomically smooth terraces are ascribed to adsorbed contaminants on the electrode. Short-term electrochemical cycling of the electrode between 1.3 and -0.2 V vs SCE in 1 M HClO₄ causes disappearance of the ripples, signaling removal of adsorbates. However, more extensive cycling causes considerable roughening of the electrode surface. Ripples are also found during scans of Pt surfaces immersed in *n*-heptane upon addition of ethyl acetate as an adsorbate. Scans of Pt surfaces immersed in aqueous solutions are also reported.

We discuss here studies of Pt electrode surfaces in air and immersed in solvent involving different types of Pt and different pretreatments by the recently developed technique of scanning tunneling microscopy (STM) (1, 2). Surface defects, including sites for chemical contamination and geometric irregularities, are often considered to be active sites for many physical and chemical processes, such as adsorption, electrodeposition, and electrocatalysis. Despite the importance of these processes and their close relationship to active sites, our understanding of atomic and near-atomic (ultramicroscopic) structures of surfaces, especially those in contact with the gas or liquid phase, is usually phenomenological. For single-crystal surfaces, low-energy electron diffraction (LEED) is one of the most commonly used techniques to monitor the long-range order and cleanliness of surfaces in ultrahigh vacuum (UHV). For polycrystalline, amorphous, or inhomogeneous surfaces, the techniques available with sufficiently high lateral resolution and vertical sensitivity are limited. Scanning electron microscopy (SEM) is useful for studying relatively large structures with a typical resolution of 100 Å. Transmission electron microscopy (TEM) has a lateral resolution of ≥ 2 Å, but it is not a surface probe and requires UHV and rather stringent sample preparation requirements, although it is extremely useful for the investigation of the morphology and microstructure of appropriate thin films. Optical techniques for *in situ* electrode surface studies exist (e.g., infrared and surface enhanced Raman spectroscopy), but they are capable of only limited spatial (lateral or vertical) resolution, as governed by diffraction limitations and source beam size. Indeed, most information about the nature of electrode surfaces in solution is obtained indirectly, for example, by noting the effects of pretreatments or adsorption on the faradaic response or double layer capacitance.

The power and potential of STM have been demonstrated recently by Binnig and Rohrer and their colleagues (1, 2). This instrument possesses simultaneously high lateral (≥ 2 Å) and vertical (≥ 0.1 Å) resolution and furnishes three-dimensional, real space images of the surface of solid materials. While most STM investigations have studied samples in UHV, several have shown the possibility of its application in air (3-6) and

liquids (7-9). Work in our laboratory has been devoted to exploring the potential application of STM in electrochemistry. Its unique capability of obtaining structural information at the atomic or near-atomic level makes it ideally suited to the study of chemical and electrochemical processes on the surface of an electrode.

Definition of surface structure is crucial to an understanding of the specific physical and chemical properties of electrodes. Electrochemistry on well-defined (usually single-crystal) surfaces depends strongly upon the cleanliness and order of the surface (10). For example, experiments in which platinum single-crystal electrodes were prepared and subjected to various treatments illustrate these effects (11-18).

As noted above, Pt is one of the most extensively studied electrode materials, and techniques for the preparation of single crystal and other forms are highly developed. However, information on the ultramicrography of these electrodes in air or liquids is still quite limited. We are interested in how various preparation techniques, especially those not requiring UHV methodology, affect the cleanliness and ultramicrostructure of the Pt surface, since most of our electrochemical and STM experiments are carried out in air or other gaseous media or in various liquids at atmospheric or reduced pressure. We seek to address the following questions here, and in following papers. (1) How smooth are the electrode surfaces? (2) How do different pretreatments affect the surface structure? (3) Can adsorption, e.g., of organic species, be detected by STM, and what is the distribution of such adsorbates? We report here our first results on STM experiments for various Pt specimens and demonstrate how pretreatment and cleanliness of the sample affect the STM images. These results are compared with SEM micrographs in some cases.

In the first part of this paper, we compare the STM images taken in air of several different types of Pt samples (single crystal or polycrystalline) after different treatments. In the next part we demonstrate the effect of ethyl acetate adsorption on the STM images of Pt in *n*-heptane. In the last part we compare the STM images of polycrystalline Pt and Pt thin films on mica obtained in H₂O with those taken in air.

EXPERIMENTAL SECTION

Preparation of the Pt Electrodes. Platinum electrodes were prepared by the procedures described previously (19-21). Polycrystalline Pt electrodes were smoothed with successive grades of wet emery paper and polished with 5-, 1-, and 0.25-μm diamond compounds and finally with 0.05-μm alumina. The polished Pt was then successively sonicated with acetone, methylene chloride, methanol, and Millipore reagent water. The oriented Pt(100) surface was prepared by following standard procedures (10, 22) and polished as described above. Several different procedures were also used for further treatment of these polished electrodes: (a) oxidation-reduction voltammetric cycles between 1.3 and -0.2 V vs SCE in 1 M HClO₄; (b) prolonged annealing (ca. 30 min) at 1000-1100 °C under argon and then cooling slowly to room temperature; (c) prolonged annealing (ca. 30 min) at 1000-1100 °C under hydrogen and then cooling slowly to room temperature; (d) annealing in I₂ vapor (ca. 1 min) at 600-700 °C under N₂ after oxidation-reduction voltammetric cycles in 1 M HClO₄ and then cooling slowly to room temperature with I₂-containing N₂ flowing;

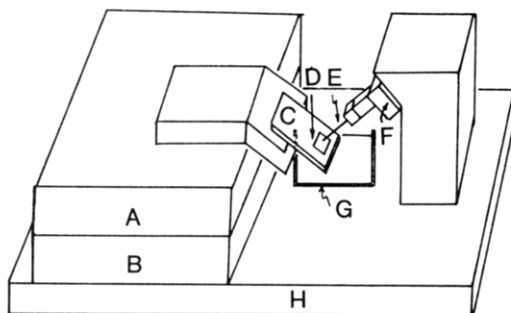


Figure 1. Schematic diagram of the STM used in this study: (A, B) X-Y stages for rough and medium positioning of sample; (C) Macor or glass support for sample; (D) sample; (E) Pt or W tip; (F) piezotriod for fine positioning and scanning of the tip; (G) glass container for solution; (H) stainless-steel base plate.

(e) the annealing procedure described in (d), then transfer to an electrochemical cell where the chemisorbed iodine was replaced by carbon monoxide, which was subsequently electrooxidized from the surface (23).

APPARATUS AND TECHNIQUES

Electrochemical Apparatus. Electrochemical measurements were performed with a PAR Model 175 universal programmer, a Model 173 potentiostat, and a Model 179 digital coulometer (Princeton Applied Research Corp., Princeton, NJ). A three-compartment electrochemical cell was used in cyclic voltammetry; one compartment held a Pt counter electrode, one held the reference electrode (SCE), and one held the Pt working electrode. All electrolyte solutions were deaerated with purified N_2 , if not otherwise mentioned.

Scanning Tunneling Microscope. The STM used here is a modified version of our earlier model (7). A rough X-Y positioning system (Model IW-501/TS-100, Burleigh Instruments, Fishers, NY) and a programmable controller (Model CE-2000, Burleigh Instruments) were used for coarse positioning and to carry the sample in the direction of a metal tip at various speeds (>10 nm/s). The total working distance of each axis is ca. 2.5 cm. Three orthogonal piezoelectric elements [type 5400 (Navy type I), Channel Industries, Inc., Santa Barbara, CA], or PZT-5A (Vernitron, Bedford, OH), were used for the fine scanner of the tip and are mounted on a stainless steel support attached to the microscope base plate (Figure 1). The sample is oriented at a 45° angle and glued on a Macor or glass support. A Pt wire sparkwelded to the Pt sample was used as the electrical contact. The microscope is oriented vertically atop five, ca. 6.5 mm thick, aluminum plates separated by Viton spacers (24). The whole system is placed on an air table (Model NRC XJ-A, Newport Corp., Fountain Valley, CA) to provide vibrational decoupling from the floor and is covered by a large Cu screen Faraday cage and a Plexiglas box to minimize electrical interference, acoustic noise, and thermal drifts. The submicrometer Pt tip was constructed and etched by procedures reported previously (7). A similar procedure was used to construct the W tip from 25- μm W wire (Alfa Products) and small glass capillary. The glass-sealed W tip was trimmed by electrochemical etching in 6 M aqueous NaOH solution. Both Pt and W tips have a radius of curvature of less than 0.1 μm , as estimated by SEM (Figure 2).

The feedback control electronics for monitoring the tunneling current and controlling the Z-piezoelectric drive are functionally similar to those of Golovchenko (25) and Drake et al. (26). Figure 3 shows a schematic illustration of the main features of the STM. The X- and Y-piezo, which have sensitivities of 1.5 $\text{\AA}/\text{V}$, serve as the scanning elements for the tip, while the Z-piezo (sensitivity, 2.8 $\text{\AA}/\text{V}$) is part of the feedback loop that keeps the current constant at a given bias voltage between the tip and sample. The current is amplified

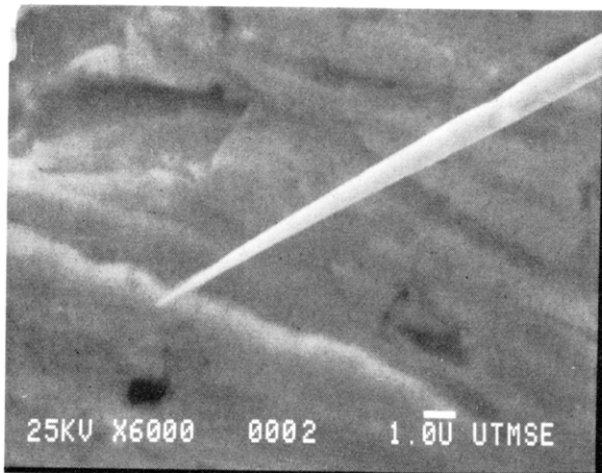


Figure 2. SEM micrographs of a Pt tip.

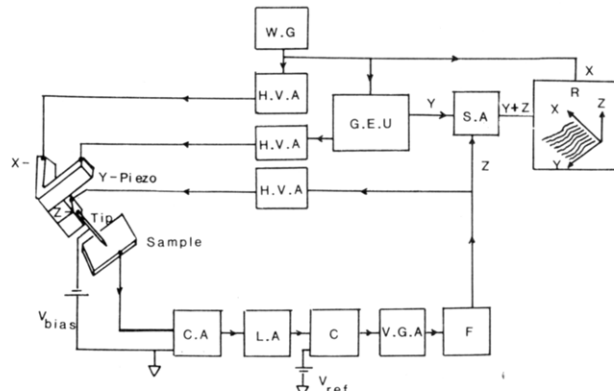


Figure 3. Block diagram of the main features of the STM: C.A., current amplifier; L.A., logarithmic amplifier; C, comparator; V.G.A., variable gain amplifier; F, filter; H.V.A., high-voltage amplifier; W.G., waveform generator; G.E.U., graphics enhancement unit; S.A., summing amplifier; R, recorder.

first through a custom-built current amplifier with a bandwidth of ca. 20 kHz and noise level <0.5%. The amplified signal, either by direct means or after further amplification by a logarithmic amplifier (Model Log 100, Burr Brown, Tucson, AZ) to linearize the feedback loop, is converted to a voltage (after comparison with a reference current) through a current-to-voltage converter. After the signal is filtered (RC time constant 2–100 ms), it is fed to a programmable high-voltage amplifier (Model PZ-70 M, Burleigh Instruments, Fishers, NY), which delivers the signal to the Z-piezo. An IBM

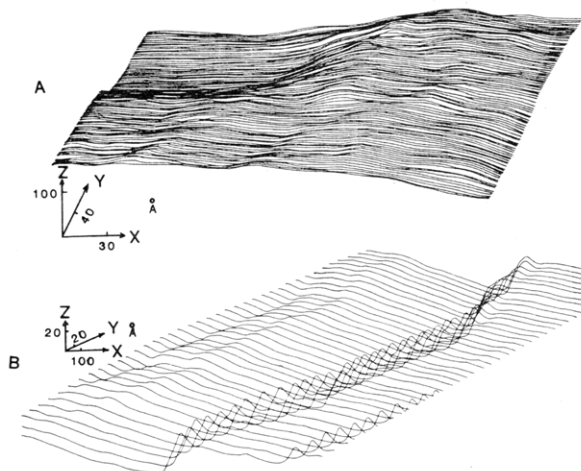


Figure 4. STM image in air of an untreated Pt foil, recorded at a tunneling current of 0.5 nA and bias voltage of 50 mV. A and B represent the images taken at two different locations.

waveform function generator from an IBM EC 225 potentiostat coupled with a custom-built graphics enhancement unit to a Houston X-Y recorder was used both for the supply of proper adjustable ramp scanning signals for the X- and Y-piezo and for the automatic plotting of the three-dimensional topograph on the recorder. No additional filters were used in the data acquisition system. We have found that the feedback control response is sufficient that we can drive the Model IW-501/TS-100 translator to carry the sample slowly to the probe tip to initiate tunneling without accidentally crashing the tip. The STM images were typically recorded at an X scan rate of 100 Å/s and Y steps of 2–3 Å.

A digital computer (IBM-AT) controlled version of this STM for programmed drive of the piezo's and data acquisition is also available, but all data shown in this paper were obtained on the analog instrument with no image enhancement or subsequent treatment of the recorder tracings.

Chemicals. All chemicals were reagent grade and were used without further purification. All aqueous solutions were prepared from a Millipore water reagent system (resistance > 18 MΩ). For air-sensitive experiments, the solution was thoroughly purged with prepurified nitrogen, and the cell chamber was kept under an atmosphere of nitrogen during the experiment.

RESULTS AND DISCUSSION

In applying the STM in studies of the kind described below, one must be aware of certain limitations of the technique. (1) It is not possible to look at the same area of the sample before and after a given treatment. Indeed, it is generally not even possible to return to the same position on the sample after the tip has been moved to a different location. There are slow drifts in the piezoelectric elements, tip, and sample (caused by temperature changes, mechanical relaxation, and hysteresis) that do not allow correlation of the voltages applied to the piezoelectric elements to a given absolute tip position after a few minutes. Recall that a STM scan encompasses an area of about 10^{-11} cm^2 (STM scans are typically 10 nm × 10 nm to 50 nm × 50 nm); an electrode of 0.01 cm^2 area would have 10^9 such scan areas. Even if these could be searched at the rate of 10 s/scan area, over 300 years would be required to look at all areas! (2) Even for samples that have been carefully pretreated, different areas of the same sample in air or under solvent display different images, i.e., even well-prepared surfaces can be quite heterogeneous. This is caused by adventitious adsorption of unavoidable impurities, surface defects, scratches and different surface structures. (3) Artifacts can arise from changes that sometimes occur in the tips. Thus after a given treatment several STM scans were taken at

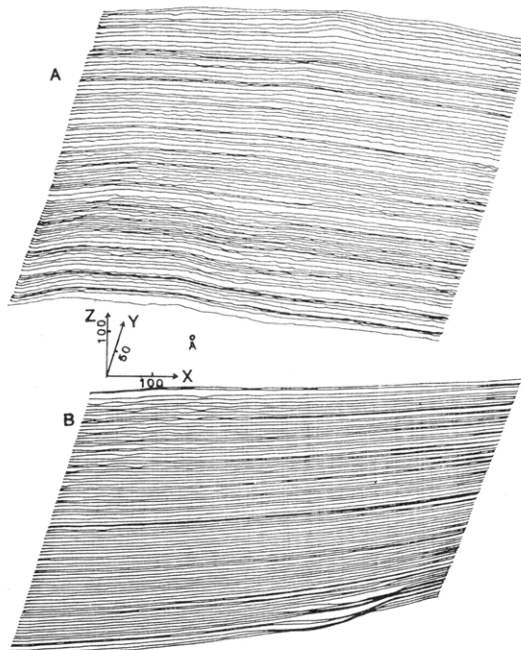


Figure 5. STM images in air of a well-polished and solvent-cleaned Pt foil (A) and the same sample after short-term (ca. 10 min) electrochemical cycling at 0.1 V/s between 1.3 and -0.2 V vs SCE in 1 M HClO_4 (B); imaging conditions, same as Figure 4.

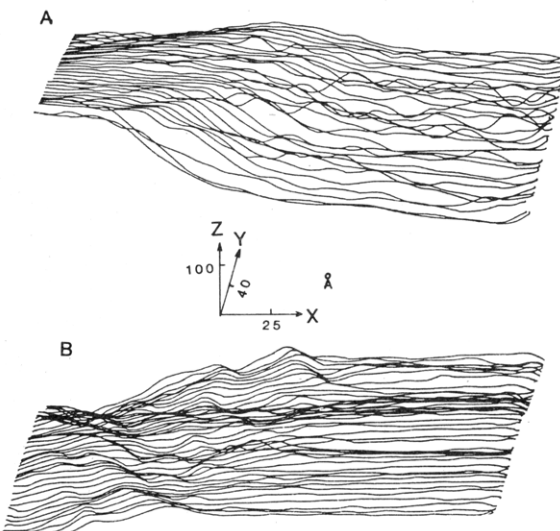


Figure 6. STM images in air of the sample used in Figure 5B after annealing in I_2 vapor at 600–700 °C for ca. 1 min. A and B represent two different locations. Imaging conditions are given in Figure 4.

different locations on the surfaces. Those we show are what we consider typical of that surface, i.e., that are found most frequently. We will, however, illustrate the different types of features that are found on the same surface at different locations, e.g., to demonstrate the degree of surface heterogeneity or adsorption sites.

STM Imaging in Air. Polycrystalline Pt Foil. We compare Pt foils subjected to three different pretreatments: type A, untreated, as received from Alfa Products (Figure 4); type B, mechanically polished as described in the Experimental Section (Figure 5A); type C, mechanically polished, electrochemically treated as stated in procedure a, and then I_2 -vapor annealed as stated in procedure d in the Experimental Section (Figure 6). As expected, the type B specimen is microscopically much smoother than type A specimens (compare Figures 4 and 5). One can observe grains of about 50–100 Å diameter randomly distributed over the surface of the untreated sample

as shown in the right-hand side of Figure 4A. An examination of the smoother locations at higher resolution reveals smooth terraces spaced of the order of 4–7 Å, which correspond to steps of one to two atomic layers (theoretically 3.5 and 7.0 Å, respectively) as shown on the left side of Figure 4B. On the right side are somewhat larger steps with large "overshoot" features along the edge. These sharp features exist predominantly close to or at step edges and they might be attributed to the electron distribution at sharp steps or kinks or loosely packed Pt clusters, as often observed in field ion micrographs (27). Such surface protrusions can generate higher electric fields, which promote field emission or field ionization. Such "overshoot" features have been seen a number of times with different samples and are the same for scans in either direction (i.e., for scans up or down the "cliff"). We are aware of the possibility that such "overshoot" features can arise on sharp edges, when the scanning tip has multiple points.

As shown in Figure 5A a well-polished and solvent-cleaned (i.e., type B) Pt surface is microscopically smooth. Very smooth areas, from several hundred to a thousand angstroms in diameter, are separated by large geometric defects caused by mechanical polishing. The STM images of type B samples are also characterized by clumps of small ripples scattered randomly over the surface (see, e.g., Figure 5A). Such ripples are not observed on more elaborately cleaned Pt specimens, and we attribute them to contamination of the Pt surface by adsorbed materials. After a number of oxidation-reduction voltammetric cycles between 1.3 and -0.2 V vs SCE in 1 M HClO_4 , these ripples disappear, probably signaling the removal of surface contamination by electrochemical processes (Figure 5B). However, long-term electrochemical cycling (e.g., >1 h at 0.1 V/s) results in roughening of the surface, which will be discussed in the section on STM of Pt single crystals. Thus, a well-polished and short-term electrochemically cleaned (e.g., ca. 10 min at 0.1 V/s) Pt foil shows topographs as smooth as the original well-polished foil, but without the ripples. If we anneal the Pt foil in I_2 vapor for ca. 1 min at 600–700 °C under N_2 and then cool it slowly to room temperature with I_2 -containing N_2 flowing (type C specimen), we obtain the STM image in Figure 6. Geometric defects induced by the I_2 treatment are clearly seen (e.g., left-hand side of Figure 6B). Note that the surface exhibits, in addition to these ultramicroscopically rough structures, some structureless zones (on the right-hand side of Figure 6A) where randomly noisy STM images are observed. Such structureless features of the STM image are also observed in the presence of ethyl acetate adsorption (as described below), and we attribute this effect to heavy surface contamination. Stable and highly ordered layers of iodine can adsorb on various well-defined Pt surfaces at atmospheric pressure (18). These adsorbed layers of halogen exert a strong effect on the electrochemical properties of the surface and are expected to influence other processes, such as electron tunneling, as well.

Pt Single Crystals. A well-polished Pt single crystal with the (100) surface exposed is similar to well-polished polycrystalline Pt samples and is characterized by smooth areas in the topographs, which are several hundred to one thousand angstroms in diameter (see Figure 7B); these are separated by ultramicroscopic defects, such as very fine scratches caused by polishing. A fine scratch of width ca. 500 Å is illustrated in Figure 7A. The corresponding SEM micrograph (Figure 8A), as expected, exhibits some microscopically rough structures, such as scratches, pits, etc., scattered over the whole surface.

After long-term oxidation-reduction voltammetric cycling between 1.3 and -0.2 V vs SCE at a scan rate of 100 mV/s in 1 M HClO_4 , this sample shows a cyclic voltammogram (CV) typical of a polycrystalline Pt surface (Figure 9), indicating

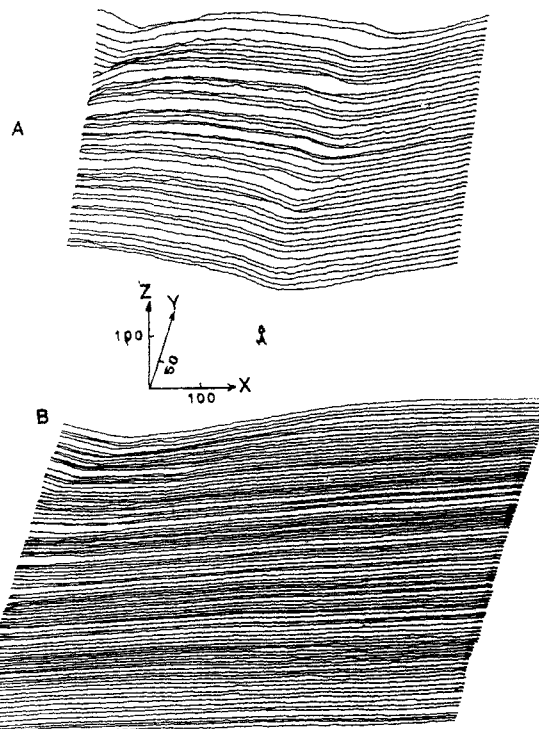


Figure 7. STM images in air of a well-polished and solvent-cleaned Pt(100) surface. A and B represent images taken at two different locations. Imaging conditions are similar to those shown in Figure 4.

that the surface has roughened considerably. This is confirmed both by SEM (Figure 8B) and by STM (Figure 10A). As shown in Figure 10A, regularly spaced mounds appear, with an average grain size of ca. 100–200 Å. This structure has also been observed by Vazquez et al. (4) on polycrystalline specimens and probably is generated by the piling up of small Pt crystallites produced through the electroreduction of the oxide layers grown in the oxidation process. Another structure we observed is depicted in Figure 10B, which shows a flat region joined by some large corrugations that might be produced from the electrochemical finishing of the sharp edges caused by mechanical polishing. Note that in contrast to long-term electrochemical cycling, which roughens the surface, short-term cycling, as discussed in the previous section, appears to clean the surface without appreciable roughening.

In Figure 11 the STM images of a well-defined Pt(100) surface prepared by the procedures of Zurawski et al. (23) are shown. Here, a well-polished Pt crystal is subjected to numerous oxidation-reduction voltammetric cycles in 1 M HClO_4 to clean and to produce a disordered surface. Cycling is stopped at 1.3 V, and the crystal is rinsed at open circuit with Millipore water. The clean and oxidized crystal is then further treated as stated in procedures d and e in the Experimental Section. The CV in 1 M HClO_4 of a Pt(100) surface after this annealing-replacement-oxidation procedure, as shown in Figure 9 (curve 2), is similar to that for a Pt(100) surface (10), suggesting that it is clean and well-ordered. The STM images indicate that in some areas (as shown in Figure 11B), the surface is smooth over a large region (several hundred to a thousand angstroms in diameter). In another area (as shown in Figure 11A), the surface is characterized by a flat terracelike region coexisting with large steps or corrugations. On one of the flat parts of the surface (as shown in Figure 11C), one can also identify mono- and diatomic steps over an atomically smooth region. By comparing Figures 10 and 11, one can see that the surface prepared from this annealing-replacement-oxidation procedure is ultramicroscopically smoother than one that simply underwent electrochemical cleaning. SEM micrographs cannot differentiate between these two specimens

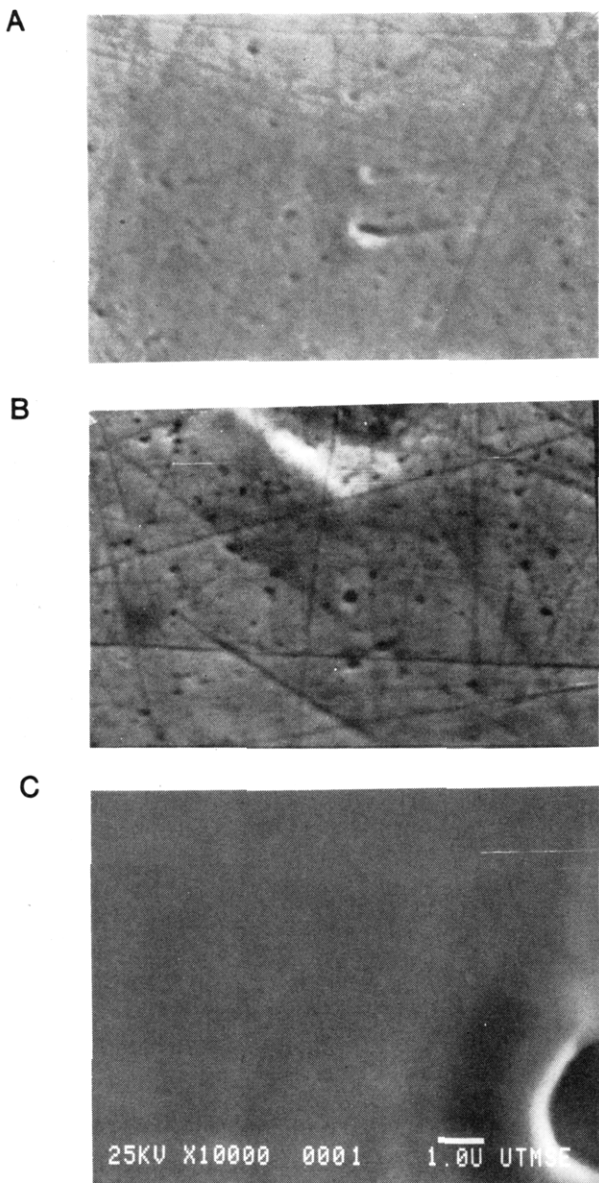


Figure 8. SEM micrographs of a Pt(100) surface: (A) mechanically polished and solvent cleaned; (B) same sample after long-term (ca. 1 h) electrochemical cycling at 0.1 V/s between 1.3 and -0.2 V vs SCE in 1 M HClO_4 ; (C) mechanically polished, solvent-cleaned, short-term (ca. 10 min) electrochemical cycling and annealed in H_2 at 1100 °C for ca. 30 min.

because of insufficient resolution. Thus STM can be used to distinguish differences in short range orderings of Pt surface atoms produced by pretreatments, which cannot be seen by SEM.

In Figures 8 and 12, we show the SEM micrograph and STM images of a well-polished, cleaned, and annealed Pt(100) surface prepared by procedures a and c described in the Experimental Section. The Pt(100) surface after short-term electrochemical cleaning is subsequently annealed to ca. 1100 °C under H_2 for ca. 30 min. A well-annealed clean Pt surface is known to reconstruct to its thermodynamically most stable state. The metastable (1 × 1) structure undergoes an irreversible reconstruction at temperatures greater than 150 °C (28). The SEM image depicted in Figure 8C clearly shows that large geometric defects caused by mechanical polishing and electrochemical etching have been flattened by the high-temperature annealing, except for the macroscopic defect shown in the lower right corner.

As shown in Figure 12B, a well-annealed clean Pt(100) surface is characterized by flat terraces, several hundred to

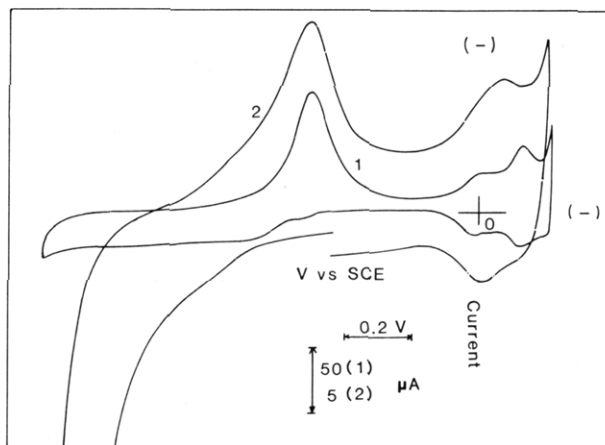


Figure 9. Cyclic voltammograms of a Pt(100) surface after long-term (ca. 1 h) electrochemical cycling at 0.1 V/s between 1.3 and -0.2 V vs SCE in 1 M HClO_4 (curve 1) and a Pt(100) surface prepared based on the procedures of Zurawski et al. (23) (curve 2). Scan rate was 0.1 V/s in 1 M HClO_4 .

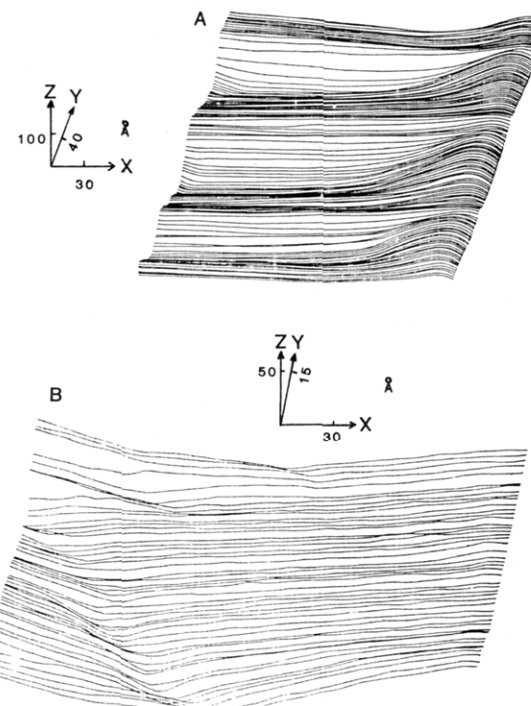


Figure 10. STM images in air of a well-polished Pt(100) surface after long-term (ca. 1 h) electrochemical processing at 0.1 V/s between 1.3 and -0.2 V vs SCE in 1 M HClO_4 . A and B represent images taken at two different locations. Imaging conditions are similar to those given in Figure 4.

a thousand angstroms in diameter, which are separated by mono- or polyatomic steps, as seen at the lower right corner of this figure. Reexamination of the flat portions of the surface by increasing the sensitivity of the feedback electronics to obtain a higher Z-axis resolution reveals the existence of periodically arranged surface corrugations on the upper portion of Figure 12C. These surface corrugations are separated by ca. 15 Å and have an average amplitude in the angstrom level. These surface corrugations might be related to the Pt (1 × 5) reconstruction structure reported by Hosler et al. (29, 30).

In addition to the smooth areas, we also sometimes observe essentially structureless ripples, such as those shown in the lower left corner of Figure 12A. This feature arises from the sample and is not an artifact of the measurement, because

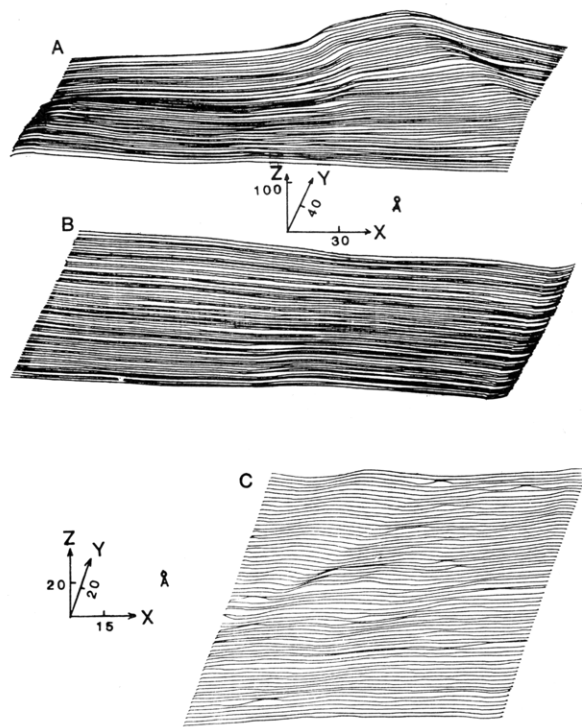


Figure 11. Surface topographs in air of a Pt(100) specimen after the annealing replacement-oxidation procedures reported by Zurawski et al. (23). A and B represent two different locations. Imaging conditions are similar to those shown in Figure 4. Image C was taken at one part of the flat surface by increasing the sensitivity of the feedback loop ca. 5 times.

it is only seen on certain locations on the surface. We also see ripples in other cases, such as with the I₂-annealed sample shown above and ethyl acetate contaminated sample, which will be illustrated in the next section. Again we ascribe these islands of oscillations to segregated chemical contamination of the surface of the sample.

STM Imaging in n-Heptane and Topographical Changes Induced by Adsorption. In a nonpolar solvent such as a saturated hydrocarbon (e.g., *n*-heptane), which probably only interacts weakly with the Pt substrate and the Pt or W tip, we are able to record STM images as clean and resolved as those recorded in air. A hydrocarbon solvent should be useful in desorbing nonpolar (hydrophobic) impurities from the Pt surface. Figure 13A shows a typical topograph of untreated Pt foil in *n*-heptane. When the solvent is changed to one with a higher dielectric constant and with both hydrophilic and hydrophobic groups attached to it, such as ethyl acetate, only spiky or oscillating images, not indicative of surface structure, are obtained (Figure 13G). Presumably ethyl acetate adsorbs fairly strongly on Pt from heptane solution through the polar carboxylate group, which is surrounded by the nonconductive, hydrophobic alkyl groups; this adsorbed species then affects the tunneling process. Dynamic processes, such as the surface diffusion of adsorbed species and adsorption/desorption kinetics, might also play roles in producing the observed oscillating image. To demonstrate the role of surface adsorption, we systematically changed the concentration of ethyl acetate in *n*-heptane and recorded the STM images at several locations to identify a typical surface pattern. As shown in Figure 13B, no significant change in the STM image was observed upon the addition of $\leq 0.06\%$ ethyl acetate (by volume) into *n*-heptane. When the concentration of ethyl acetate was increased to ca. 0.1%, the STM image started to exhibit ripples in selected locations superimposed on the typical structure for untreated Pt foil (see Figure 13D). These ripples are apparently not due to adsorbate-induced

reconstruction of the Pt surface as observed by Hosler et al. (29), which concern CO-induced topographical changes on Pt, since, after their appearance, we can recover the clean image by washing the sample very thoroughly with *n*-heptane. The number of ripples increases with the concentration of ethyl acetate, and they are preferentially segregated on particular locations (see the lower left corner of Figure 13E,F). The adsorbed species probably nucleate and form patches on the surface because of lateral interactions between the adsorbate particles. We frequently see such "adsorption patches" on surfaces (e.g., Figures 12A, 13E,F, and 14B).

STM Imaging in H₂O. As mentioned in the introduction, one of the major goals of this project is to explore the potential application of the STM of electrodes *in situ*. Since water is one of the most commonly used solvents in electrochemical studies, we chose it as the first electrochemical liquid medium for STM study. To test the applicability of our STM for samples immersed in H₂O, we obtained topographs of untreated Pt foil and Pt thin film on mica and compared these to those obtained in air. The STM patterns of an untreated Pt foil imaged in H₂O (Figure 14A) are very similar to those recorded in air (Figure 4A). Similar grains (50–100 Å in diameter), which are randomly distributed on the surface, can easily be identified on both images. As a second test sample, we chose a smooth Pt thin film coated on atomically smooth mica sheet. As shown in Figure 14C, its surface is much smoother than the untreated Pt foil shown above. In air (Figure 14B) we can also clearly observe some fairly large oscillations or ripples on the right side of this image. Those corrugations are separated too far (30–40 Å) and have too high an amplitude (ca. 4 Å) to be attributed to the (1 × 5) reconstruction structure; again we think they represent adsorbed species on the electrode. The STM image in H₂O of the same sample (but not at the same location) (Figure 12C) clearly shows that its surface is much smoother than an untreated Pt foil.

The imaging of the topograph of Pt samples in H₂O, as shown above, seems possible. However, no atomic resolution has been reached so far, although Sonnenfeld and Hansma (8) have recently shown that the STM can operate with atomic resolution on graphite in water. We have noticed that the introduction of H₂O into the system not only suppresses the noise level by damping vibrations but also smears out very fine structures usually observable in air. Besides, for samples in H₂O, there exists a very slowly fluctuating signal (<1 Hz), which is not observed in air. We are currently unable to carry out STM scans with an electrochemical reaction occurring on the substrate, because the much larger faradaic (and non-faradaic) currents (compared to the nanoampere-level tunneling currents) perturb the feedback control system in the STM. This problem is probably addressable by a suitable change in the instrumentation.

CONCLUSIONS

STM has been shown to be useful in assessing the structural variations of Pt specimens prepared by different procedures. The resolution in air is such that mono- and diatomic steps can be observed on untreated Pt foil; this surface also contains numerous grains 50–100 Å in diameter. Short-term oxidation-reduction voltammetric cycles in 1 M HClO₄ clean the Pt surface without roughening it appreciably. Long-term electrochemical processing, similar to that observed by Vazquez et al. (4), on polycrystalline Pt samples, generates a pebblelike structure on a single-crystal Pt specimen. Clean and atomically smooth Pt(100) surfaces, several hundred to a thousand angstroms in diameter can be prepared by the annealing-replacement-oxidation procedure reported by Zurawski et al. (23). However, I₂-vapor annealing alone probably leads to the formation of small grains at certain locations (see

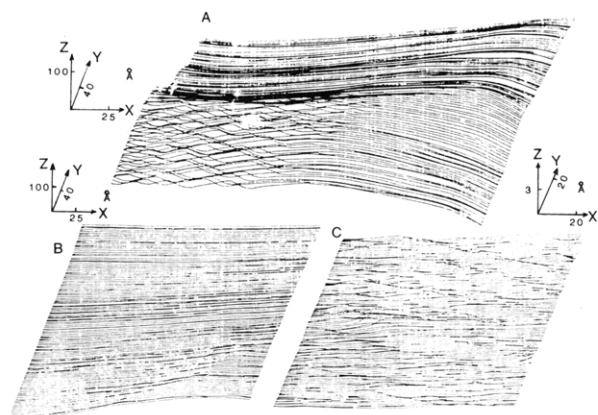


Figure 12. Surface topographs in air of a Pt(100) surface, well-cleaned and annealed to ca. 1100 °C under H₂ for ca. 30 min. A and B represent two images at two different locations. Image C was obtained from one part of the flat surface by increasing the sensitivity.

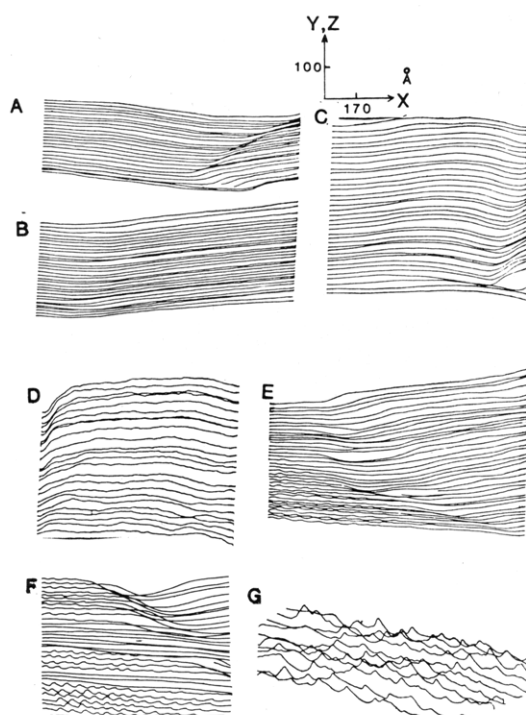


Figure 13. STM images of an untreated Pt foil in n-heptane, containing different concentrations of ethyl acetate: A, 0%; B, 0.02%; C, 0.06%; D, 0.1%; E and F, 0.6%; G, 100% ethyl acetate. Images were recorded at a constant current of 0.5 nA and bias voltage of 50 mV.

Figure 6B). I₂ can also strongly adsorb on the surface of Pt and influence its STM image. A clean and atomically smooth Pt(100) surface can also be prepared by annealing a well-polished and cleaned specimen under H₂, although atomic corrugations are observed on some locations of this sample. Chemical contamination (e.g., the adsorption of organics) on the Pt surface results in a ripplelike pattern in the STM image. This effect was found, for example, in STM images for a Pt surface immersed in n-heptane with different concentrations of ethyl acetate. Adsorbed species seem to form local patches rather than be distributed randomly over the surface. One can reasonably account for such behavior by the stronger interaction among adsorbed species on the surface compared with interactions with adsorbed solvent molecules. Hence adsorption of organics may follow a nucleation and growth pattern, in a manner analogous to that frequently found for metal deposition. We have also demonstrated the applicability

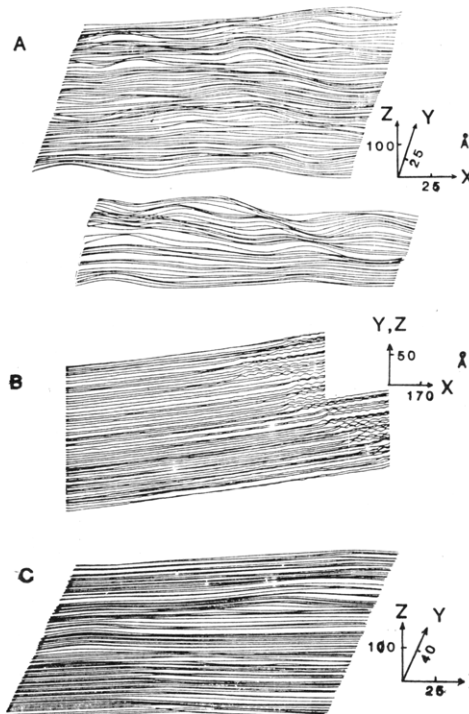


Figure 14. STM patterns of an untreated Pt foil imaged in H₂O at an average current of ca. 2 nA and a bias voltage of 100 mV. (B) Surface topograph of Pt thin film (1.8 μm) on a mica sheet imaged in air at an average current of ca. 0.5 nA and a bias voltage of 50 mV. (C) Same sample as in B but imaged in H₂O at an average current of ca. 2 nA and a bias voltage of 100 mV. Pt tip was used in H₂O and W (or Pt) tip was used in air.

of our STM to the imaging of surfaces of Pt samples in H₂O.

Registry No. I₂, 7553-56-2; Pt, 7440-06-4; H₂, 1333-74-0; HClO₄, 7601-90-3; ethyl acetate, 141-78-6.

LITERATURE CITED

- Binnig, G.; Rohrer, H. *Helv. Phys. Acta* **1982**, *55*, 726.
- Binnig, G.; Rohrer, H. *Surf. Sci.* **1983**, *126*, 236.
- Drake, B.; Sonnenfeld, R.; Schneir, J.; Hansma, P. K.; Slough, G.; Coleman, R. V. *Rev. Sci. Instrum.* **1986**, *57*, 441.
- Vazquez, L.; Gomez, J.; Baro, A. M.; Garcia, N.; Marcos, M. L.; Gonzalez Velasco, J.; Vara, J. M.; Arvia, A. J.; Presa, J.; Garcia, A.; Aguilar, M. J. *Am. Chem. Soc.* **1987**, *109*, 1730.
- Park, S.-I.; Quate, C. F. *Appl. Phys. Lett.* **1986**, *48*, 112.
- Morita, S.; Itaya, K.; Mikoshiba, N. *Jpn. J. Appl. Phys.* **1986**, *25*, L743.
- Liu, H.-Y.; Fan, F.-R. F.; Lin, C. W.; Bard, A. J. *J. Am. Chem. Soc.* **1986**, *108*, 3838.
- Sonnenfeld, R.; Hansma, P. K. *Science* **1986**, *232*, 211.
- Sonnenfeld, R.; Schardt, B. C. *Phys. Lett.* **1986**, *49*, 1172.
- Hubbard, A. T. *Acc. Chem. Res.* **1980**, *13*, 177, and references therein.
- Ross, P. N., Jr. *J. Electroanal. Chem.* **1977**, *76*, 139.
- O'Grady, W. E.; Woo, M. Y. C.; Hagans, P. L.; Yeager, E. J. *J. Vac. Sci. Technol.* **1977**, *14*, 365.
- Will, F. *J. Electrochem. Soc.* **1965**, *112*, 451.
- Yamamoto, K.; Kolb, D. M.; Kotz, R.; Lehmpfuhl, G. *J. Electroanal. Chem.* **1979**, *96*, 233.
- Conway, B. E.; Angerstein-Kozlowska, H.; Ho, F. C. *J. Vac. Sci. Technol.* **1977**, *14*, 351.
- Claviller, J.; Faure, R.; Guinet, G.; Durand, R. *J. Electroanal. Chem.* **1980**, *107*, 205.
- Aberdam, D.; Durand, R.; Faure, R.; El-Omar, F. *Surf. Sci.* **1986**, *171*, 303.
- Wieckowski, A.; Schardt, B. C.; Rosasco, S. D.; Stickney, J. L.; Hubbard, A. T. *Surf. Sci.* **1984**, *146*, 115.
- Soriaga; Hubbard, A. T. *J. Am. Chem. Soc.* **1982**, *104*, 2735.
- Soriaga, M. P.; Hubbard, A. T. *J. Am. Chem. Soc.* **1982**, *104*, 3937.
- Hubbard, A. T.; Ishikawa, R. M.; Katekaru, J. *J. Electroanal. Chem.* **1978**, *86*, 271.
- Behm, R. J.; Thiel, P. A.; Norton, P. R. Ertl, G. *J. Chem. Phys.* **1983**, *78*, 7437.
- Zurawski, D.; Rice, L.; Hourani, M.; Wieckowski, A. *J. Electroanal. Chem.*, in press.

- (24) Gerber, C.; Binnig, G.; Fuchs, H.; Marti, O.; Rohrer, H. *Rev. Sci. Instrum.* 1986, 57, 221.
- (25) Golovchenko, J. A. *Science* 1986, 232, 48.
- (26) Drake, B.; Sonnenfeld, R.; Schneir, J.; Hansma, P. K.; Slough, G.; Coleman, R. V. *Rev. Sci. Instrum.* 1986, 57, 441.
- (27) Ehrlich, G. *Phys. Today* 1981 (June), 44.
- (28) Heinz, K.; Lang, E.; Strauss, K.; Muller, K. *Appl. Surf. Sci.* 1982, 11/12 611.
- (29) Hosler, W.; Behm, R. J.; Ritter, E. *IBM J. Res. Dev.* 1986, 30, 403.
- (30) Behm, R. J.; Hosler, W.; Ritter, E.; Binnig, G. *J. Vac. Sci. Technol., A* 1986, 4, 1330.

RECEIVED for review August 3, 1987. Accepted December 30, 1987. The support of the Robert A. Welch Foundation (F-079) and the Texas Advanced Technology Research Program is gratefully acknowledged.

Potentiometric and Thermal Studies of a Coated-Wire Antazoline-Selective Electrode

Sayed S. Badawy,* Adel F. Shoukry, and Mohamad M. Omar

Department of Chemistry, Faculty of Science, University of Cairo, Giza, Egypt

A coated-wire antazoline-selective electrode based on incorporation of antazoline-tetraphenylborate ion pair in a poly(vinyl chloride) coating membrane was constructed. The influences of membrane composition, temperature, pH of the test solution, and foreign ions on the electrode performance were investigated. The electrode showed a Nernstian response over an antazoline concentration range of 1.41×10^{-5} to 0.89×10^{-2} M, at 25 °C and was found to be very selective, precise, and usable within the pH range 2.3–9.0. The standard electrode potentials, E° , were determined at 20, 25, 30, 35, 40, and 45 °C and used to calculate the isothermal temperature coefficient (dE°/dT) of the electrode. Temperatures higher than 45 °C affect seriously the electrode performance. The electrode was successfully used for potentiometric determination of antazoline hydrochloride both in pure solutions and in pharmaceutical preparations.

Antazoline is an ethylenediamine derivative with the properties and uses of antihistamines. It has local anaesthetic and also some anticholinergic properties. It is less irritating to the tissues than most other antihistamines. It has been used by mouth in the prevention and treatment of cardiac arrhythmias and administrated by intramuscular or slow intravenous injection.

Several methods have been reported for the determination of this important compound, including spectrophotometric (1–4), fluorometric (5), polarographic (6, 7), gravimetric (8), titrimetric (9), NMR spectrophotometric (10), and chromatographic (11) methods. However, most of these methods involve several manipulation steps before the final result of the analysis is obtained. Although potentiometric methods of analysis using ion-selective electrodes are simple, cheap, applicable to samples of different natures, and usable with automated systems, no selective electrode is, so far, available for the determination of antazoline.

The present work, thus, describes a new selective membrane electrode of the coated wire type, for determination of antazoline in pure solutions and in pharmaceutical preparations. This electrode is based on incorporation of an ion-pair complex of tetraphenylborate anion (TPB⁻) with antazoline cation (AnH⁺) in poly(vinyl chloride) matrix.

It is noteworthy that all previously reported investigations using poly(vinyl chloride), PVC, membrane selective electrodes for determination of species of pharmaceutical and/or medical

importance have been carried out at only one temperature, mostly 20 or 25 °C. No attention was paid to the higher temperature range, 25–45 °C, although many potentiometric measurements concerning biological media and fluids (12) are made at such a temperature range. In this paper, the effect of temperature of the test solution on the performance characteristics of the proposed coated-wire electrode (CWE) is reported.

EXPERIMENTAL SECTION

Reagents and Materials. All chemicals used were of analytical or pharmacopeial grade (can be used for manufacturing pharmaceutical preparations). Bidistilled water was used throughout all experiments. The pharmaceutical preparations containing antazoline (Antazoline tablets, Calazol lotion, and Antistine-Privine drops) were obtained from local drug stores. The AnH-TPB ion pair was prepared by a method similar to that described before (13). The base component of the produced ion pair has been determined by the nonaqueous titration method published earlier (14). The agreement between calculated and found values was very good confirming the postulated stoichiometry, the 1:1 (AnH:TPB) molar ratio. This stoichiometry was also confirmed by elemental analysis.

Construction of Electrode. Spectroscopic pure copper wires of 2.0 mm diameter and 12 cm length were tightly insulated by polyethylene tubes leaving 1.0 cm at one end for coating and 0.5 cm at the other end for connection. The coating solutions were prepared by dissolving varying amounts of powdered PVC, dioctyl phthalate, DOP (plasticizer), and the AnH-TPB in the least amount of tetrahydrofuran possible (3–4 mL), Table I. Prior to coating, the polished copper surface was washed with a detergent and water, thoroughly rinsed with deionized water, and dried with acetone. Then the wire is rinsed with chloroform and allowed to dry. Afterward, the copper wire was coated by quickly dipping it into the coating solution, A, B, C, or D several times and allowing the film left on the wire to dry in air for about 2 min. The process was repeated several times until a plastic membrane of approximately 1.0 mm thickness was formed as measured by an electronic linear measuring gauge head, Tesa-GT 41. The prepared electrodes were preconditioned by soaking them for 1.5 h in 10^{-3} M AnHCl solution.

Potentiometric Studies and Electrochemical System. Potentiometric measurements were carried out with a Chemtrix type 62 digital pH/mV meter. A Techne circulator thermostat, Model C-100, was used to control the temperature of the test solution. The electrochemical system was as follows: Cu|membrane|test solution||KCl salt bridge||KCl(sat.)|Hg₂Cl₂–Hg.

Construction of the Calibration Graphs. Suitable increments of standard AnHCl solution were added to 50 mL of 10^{-6} M AnHCl solution so as to cover the concentration range 10^{-6} to